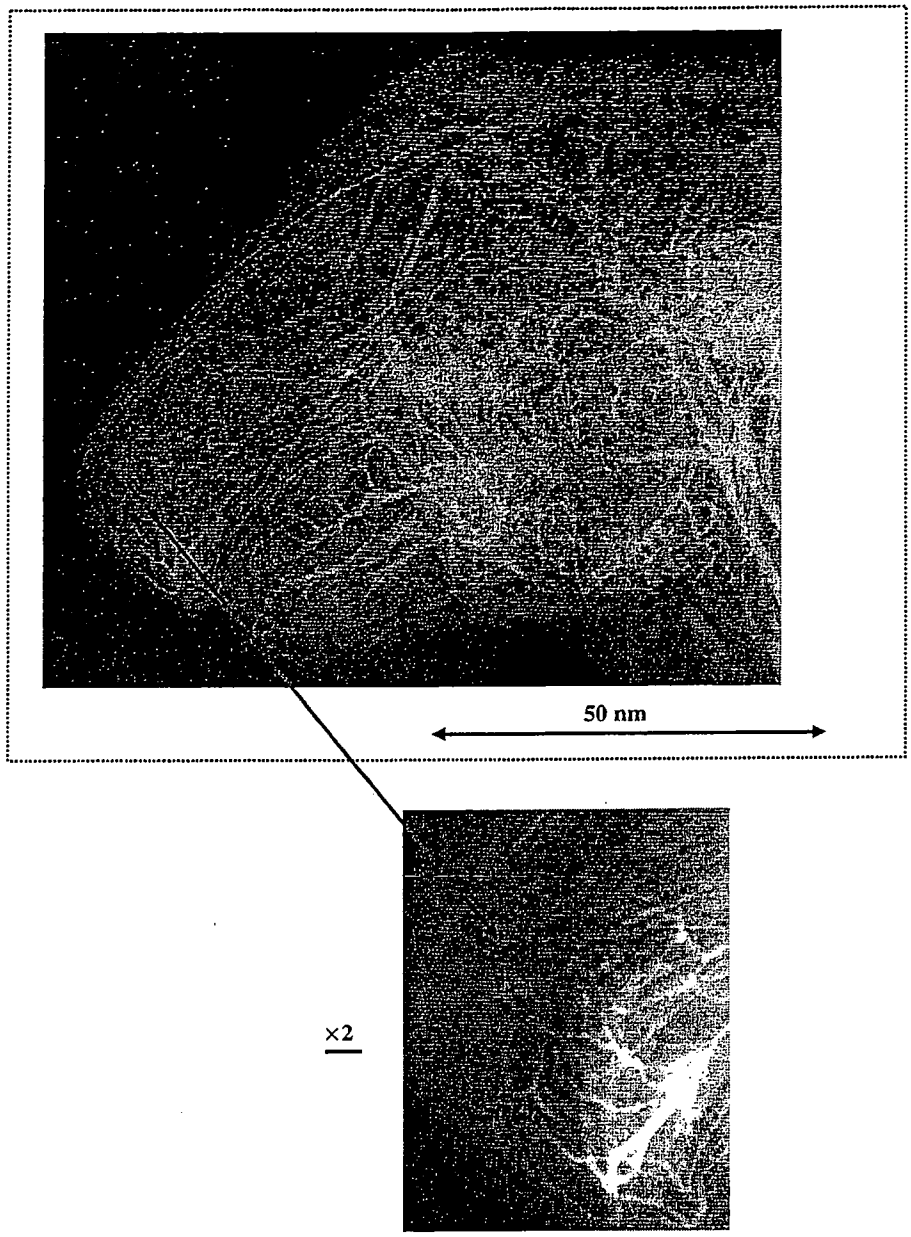

Fig. 12. Angiography of a rabbit head using gadolinium oxide powder.

The image of water (20% gadolinium oxide suspension) falling into a polypropylene beaker from a plastic test tube is shown in Fig. 9. The diameter of gadolinium oxide powder ranges from 1 to 10 μm. Because the X-ray duration was about 100 ns, the stop-motion image of water could be obtained.

Fig. 10 shows an angiogram of a polytetrafluoroethylene (Teflon) tube in a PMMA case using a contrast medium which contains approximately 65% gadodiamidehydrate, and a high-contrast tube with a bore diameter of 1.0 mm is observed. Figs. 11 and 12 show angiograms of a rabbit ear and head using gadolinium oxide powder, and fine blood vessels of approximately 100 μm were visible.

6. Conclusions and outlook

In summary, we succeeded in producing K_α rays of tungsten and in performing K-edge angiography using gadolinium contrast media with a K-edge of 50.2 keV, and this K-edge angiography could be a useful technique

to decrease the dose absorbed by patients. Although we employed tungsten K_α (58.9 keV) rays, L-series characteristic rays should be absorbed before angiography using a filter.

We obtained sufficient X-ray intensity for CR angiography with X-ray durations of approximately 100 ns, and the intensity can be increased by increasing the charging voltage at a constant target–cathode space. In an empirical equation, because the characteristic X-ray intensity is proportional to approximately 1.5th power of the voltage difference between the tube voltage and the critical excitation voltage, optimum intensity for angiography can be controlled. In this research, the generator produced instantaneous number of K photons was approximately 1×10^9 photons/cm^2 per pulse at 1.0 m from the source.

Because the dimensions of the X-ray source are primarily determined by the target diameter, the diameter should be minimized in order to improve the spatial resolution, and can be reduced to approximately 0.5 mm. Subsequently, the sampling pitch can be decreased to 43.8 μm using a CR system (Konica Minolta Regius 190) to observe fine blood vessels of approximately 50 μm diameter.

Using this flash X-ray generator, enhanced K-edge angiography using iodine contrast media can also be performed using a cerium target. In addition, steady-state monochromatic X-rays can be produced by a similar tube utilizing a hot cathode and a constant high-voltage power supply. In addition, fine focusing can be realized using tungsten or molybdenum target, and these X-ray generators could be employed to perform quasi-monochromatic phase-contrast radiography for edge enhancement.

Acknowledgments

This work was supported by Grants-in-Aid for Scientific Research (13470154, 13877114, 16591181 and 16591222) and Advanced Medical Scientific Research from MECSST, Health and Labor Sciences Research Grants (RAMT-nano-001, RHGTEFB-genome-005 and RHGTEFB-saisei-003), grants from the Keiryo Research Foundation, the Promotion and Mutual Aid Corporation for Private Schools of Japan, the Japan Science and Technology Agency (JST) and the New Energy and Industrial Technology Development Organization (NEDO, Industrial Technology Research Grant Program in 2003).

References

Ando, M., Maksimenko, M., Sugiyama, H., Pattanasiriwisawa, W., Hyodo, K., Uyama, C., 2002. A simple X-ray dark- and bright-field imaging using achromatic Laue optics. Jpn. J. Appl. Phys. 41, L1016–L1018.

Davis, T.J., Gao, D., Gureyev, T.E., Stevenson, A.W., Wilkins, S.W., 1995. Phase-contrast imaging of weakly absorbing materials using hard X-rays. Nature 373, 595–597.

Hyodo, K., Ando, M., Oku, Y., Yamamoto, S., Takeda, T., Itai, Y., Ohtsuka, S., Sugishita, Y., Tada, J., 1998. Development of a two-dimensional imaging system for clinical applications of intravenous coronary angiography using intense synchrotron radiation produced by a multipole wiggler. J. Synchrotron Rad. 5, 1123–1126.

Momose, A., Takeda, T., Itai, Y., Hirano, K., 1996. Phase-contrast X-ray computed tomography for observing biological soft tissues. Nat. Med. 2, 473–475.

Mori, H., Hyodo, K., Tanaka, E., Mohammed, M.U., Yamakawa, A., Shinozaki, Y., Nakazawa, H., Tanaka, Y., Sekka, T., Iwata, Y., Honda, S., Umetani, K., Ueki, H., Yokoyama, T., Tanioka, K., Kubota, M., Hosaka, H., Ishizawa, N., Ando, M., 1996. Small-vessel radiography in situ with monochromatic synchrotron radiation. Radiology 201, 173–177.

Sato, E., Kimura, S., Kawasaki, S., Isobe, H., Takahashi, K., Tamakawa, Y., Yanagisawa, T., 1990. Repetitive flash X-ray generator utilizing a simple diode with a new type of energy-selective function. Rev. Sci. Instrum. 61, 2343–2348.

Sato, E., Takahashi, K., Sagae, M., Kimura, S., Oizumi, T., Hayasi, Y., Tamakawa, Y., Yanagisawa, T., 1994a. Sub-kilohertz flash X-ray generator utilizing a glass-enclosed cold-cathode triode. Med. Biol. Eng. Comput. 32, 289–294.

Sato, E., Sagae, M., Takahashi, K., Shikoda, A., Oizumi, T., Hayasi, Y., Tamakawa, Y., Yanagisawa, T., 1994b. 10kHz microsecond pulsed X-ray generator utilizing a hot-cathode triode with variable durations for biomedical radiography. Med. Biol. Eng. Comput. 32, 295–301.

Sato, E., Sato, K., Tamakawa, Y., 2000. Film-less computed radiography system for high-speed imaging. Ann. Rep. Iwate Med. Univ. Sch. Lib. Arts Sci. 35, 13–23.

Sato, E., Hayasi, Y., Germer, R., Tanaka, E., Mori, H., Kawai, T., Obara, H., Ichimaru, T., Takayama, K., Ido, H., 2003a. Irradiation of intense characteristic X-rays from weakly ionized linear molybdenum plasma. Jpn. J. Med. Phys. 23, 123–131.

Sato, E., Hayasi, Y., Germer, R., Tanaka, E., Mori, H., Kawai, T., Ichimaru, T., Takayama, K., Ido, H., 2003b. Quasi-monochromatic flash X-ray generator utilizing weakly ionized linear copper plasma. Rev. Sci. Instrum. 74, 5236–5240.

Sato, E., Sagae, M., Tanaka, E., Hayasi, Y., Germer, R., Mori, H., Kawai, T., Ichimaru, T., Sato, S., Takayama, Y., Ido, H., 2004a. Quasi-monochromatic flash X-ray generator utilizing a disk-cathode molybdenum tube. Jpn. J. Appl. Phys. 43, 7324–7328.

Sato, E., Hayasi, Y., Germer, R., Tanaka, E., Mori, H., Kawai, T., Ichimaru, T., Sato, S., Takayama, K., Ido, H., 2004b. Sharp characteristic X-ray irradiation from weakly ionized linear plasma. J. Electron Spectrosc. Related Phenom. 137–140, 713–720.

Sato, E., Tanaka, E., Mori, H., Kawai, T., Ichimaru, T., Sato, S., Takayama, K., Ido, H., 2004c. Demonstration of

enhanced K-edge angiography using a cerium target X-ray generator. Med. Phys. 31, 3017–3021.

Sato, E., Tanaka, E., Mori, H., Kawai, T., Ichimaru, T., Sato, S., Takayama, Y., Ido, H., 2005a. Compact monochromatic flash X-ray generator utilizing a disk-cathode molybdenum tube. Med. Phys. 32, 49–54.

Sato, E., Tanaka, E., Mori, H., Kawai, T., Sato, S., Takayama, Y., 2005b. High-speed enhanced K-edge angiography utilizing cerium plasma X-ray generator. Opt. Eng. 44, 049001–049016.

Sato, E., Tanaka, E., Mori, H., Kawai, T., Sato, S., Takayama, Y., 2005c. Clean monochromatic X-ray irradiation from weakly ionized linear copper plasma. Opt. Eng. 44, 049002–049016.

Shikoda, A., Sato, E., Sagae, M., Oizumi, T., Tamakawa, Y., Yanagisawa, T., 1994. Repetitive flash X-ray generator having a high-durability diode driven by a two-cable-type line pulser. Rev. Sci. Instrum. 65, 850–856.

Takahashi, K., Sato, E., Sagae, M., Oizumi, T., Tamakawa, Y., Yanagisawa, T., 1994. Fundamental study on a long-duration flash X-ray generator with a surface-discharge triode. Jpn. J. Appl. Phys. 33, 4146–4151.

Thompson, A.C., Zeman, H.D., Brown, G.S., Morrison, J., Reiser, P., Padmanabahn, V., Ong, L., Green, S., Giacomini, J., Gordon, H., Rubenstein, E., 1992. First operation of the medical research facility at the NSLS for coronary angiography. Rev. Sci. Instrum. 63, 625–628.

Available online at www.sciencedirect.com
ScienceDirect
Radiation Physics and Chemistry 75 (2006) 1812–1818
Radiation Physics and Chemistry
www.elsevier.com/locate/radphyschem

Preliminary study for producing higher harmonic hard X-rays from weakly ionized nickel plasma

Eiichi Sato[a,*], Yasuomi Hayasi[a], Etsuro Tanaka[b], Hidezo Mori[c], Toshiaki Kawai[d], Takashi Inoue[e], Akira Ogawa[e], Shigehiro Sato[f], Kazuyoshi Takayama[g], Jun Onagawa[h], Hideaki Ido[h]

[a]*Department of Physics, Iwate Medical University, 3-16-1 Honchodori, Morioka 020-0015, Japan*
[b]*Department of Nutritional Science, Faculty of Applied Bio-science, Tokyo University of Agriculture, 1-1-1 Sakuragaoka, Setagaya-ku 156-8502, Japan*
[c]*Department of Cardiac Physiology, National Cardiovascular Center Research Institute, 5-7-1 Fujishirodai, Suita, Osaka 565-8565, Japan*
[d]*Electron Tube Division #2, Hamamatsu Photonics K. K., 314-5 Shimokanzo, Iwata 438-0193, Japan*
[e]*Department of Neurosurgery, School of Medicine, Iwate Medical Universichimaru, Morioka 020-8505, Japan*
[f]*Department of Microbiology, School of Medicine, Iwate Medical University, 19-1 Uchimaru, Morioka 020-8505, Japan*
[g]*Shock Wave Research Center, Institute of Fluid Science, Tohoku University, 2-1-1 Katahira, Sendai 980-8577, Japan*
[h]*Department of Applied Physics and Informatics, Faculty of Engineering, Tohoku Gakuin University, 1-13-1 Chuo, Tagajo 985-8537, Japan*

Accepted 23 November 2005

Abstract

In the plasma flash X-ray generator, a 200 nF condenser is charged up to 50 kV by a power supply, and flash X-rays are produced by the discharging. The X-ray tube is a demountable triode with a trigger electrode, and the turbomolecular pump evacuates air from the tube with a pressure of approximately 1 mPa. Target evaporation leads to the formation of weakly ionized linear plasma, consisting of nickel ions and electrons, around the fine target, and intense Kα lines are left using a 15-μm-thick cobalt filter. At a charging voltage of 50 kV, the maximum tube voltage was almost equal to the charging voltage of the main condenser, and the peak current was about 18 kA. The K-series characteristic X-rays were clean and intense, and higher harmonic X-rays were observed. The X-ray pulse widths were approximately 300 ns, and the time-integrated X-ray intensity had a value of approximately 1.0 mGy at 1.0 m from the X-ray source with a charging voltage of 50 kV.

PACS: 52.80.Vp; 52.90.+z; 87.59.Bh; 87.64.Gb

Keywords: Weakly ionized linear plasma; K-series characteristic X-rays; Clean characteristic X-rays; Higher harmonic hard X-rays

1. Introduction

In conjunction with single crystals, synchrotrons produce monochromatic parallel beams, which are fairly similar to monochromatic parallel laser beams, and the

*Corresponding author.
E-mail address: dresato@iwate-med.ac.jp (E. Sato).

0969-806X/$ - see front matter © 2006 Elsevier Ltd. All rights reserved.
doi:10.1016/j.radphyschem.2005.11.012

beams have been applied to enhanced K-edge angiography (Thompson et al., 1992; Mori et al., 1996; Hyodo et al., 1998), phase-contrast radiography (Davis et al., 1995; Momose et al., 1996; Ando et al., 2002), and crystallography. Therefore, the production of coherent hard X-ray lasers for various research projects, including biomedical applications, has long been wished for.

Recently, soft X-ray lasers have been produced by a gas-discharge capillary (Rocca et al., 1994, 1996; Macchietto et al., 1999), and the laser pulse energy substantially increased in proportion to the capillary length. These kinds of fast discharges can generate hot and dense plasma columns with aspect ratios approaching 1000:1. However, it is difficult to increase the laser photon energy to 10 keV or beyond. Because there are no X-ray resonators in the high-photon-energy region, new methods for increasing coherence will be desired in the future.

To apply flash X-ray generators to biomedicine, several different generators have been developed (Germer, 1979; Sato et al., 1990, 1994a, b; Shikoda et al., 1994; Takahashi et al., 1994), and plasma X-ray generators (Sato et al., 2003a, b, 2004a–c, 2005a–c) are useful for producing clean characteristic X-rays in the low-photon-energy region of less than 20 keV. By forming weakly ionized linear plasma using rod targets, we confirmed irradiation of intense K-series characteristic X-rays from the axial direction of the linear plasmas of nickel, copper, and molybdenum, since the bremsstrahlung X-rays are absorbed effectively by the linear plasma; monochromatic clean Kα rays were produced using K-edge filters.

In this paper, we describe a recent plasma flash X-ray generator utilizing a rod target, used to perform a preliminary experiment for generating clean K-series characteristic X-rays and their higher harmonic hard X-rays by forming a plasma cloud around a fine target.

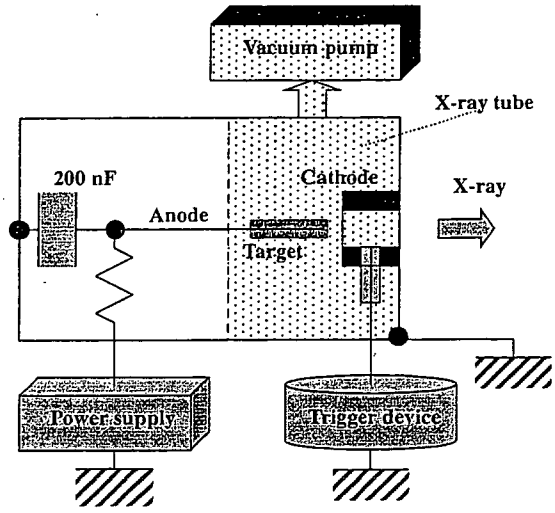

Fig. 1. Block diagram including electric circuit of the plasma flash X-ray generator.

2. Generator

Fig. 1 shows a block diagram of the high-intensity plasma flash X-ray generator. This generator consists of the following essential components: a high-voltage power supply, a high-voltage condenser with a capacity of approximately 200 nF, a turbomolecular pump, a krytron pulse generator as a trigger device, and a flash X-ray tube. The high-voltage main condenser is charged to 50 kV by the power supply, and electric charges in the condenser are discharged to the tube after triggering the cathode electrode with the trigger device. The plasma flash X-rays are then produced.

The schematic drawing of the plasma X-ray tube is illustrated in Fig. 2. The X-ray tube is a demountable

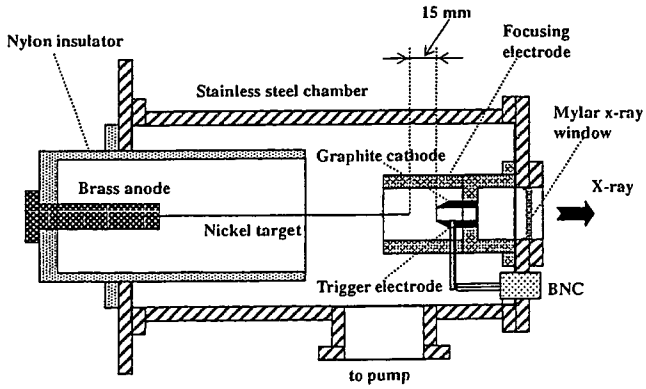

Fig. 2. Schematic drawing of the flash X-ray tube with a rod nickel target.

cold-cathode triode that is connected to the turbomolecular pump with a pressure of approximately 1 mPa. This tube consists of the following major parts: a hollow cylindrical carbon cathode with a bore diameter of 10.0 mm, a brass focusing electrode, a trigger electrode made from copper wire, a stainless steel vacuum chamber, a nylon insulator, a polyethylene terephthalate (Mylar) X-ray window 0.25 mm in thickness, and a rod-shaped nickel target 3.0 mm in diameter with a tip angle of 60°. The distance between the target and cathode electrodes is approximately 15 mm, and the trigger electrode is set in the cathode electrode. As electron beams from the cathode electrode are roughly converged to the target by the focusing electrode, evaporation leads to the formation of a weakly ionized linear plasma, consisting of nickel ions and electrons, around the fine target.

In the linear plasma, bremsstrahlung photons with energies higher than the K-absorption edge are effectively absorbed and are converted into fluorescent X-rays. The plasma then transmits the fluorescent rays easily, and bremsstrahlung rays with energies lower than the K-edge are also absorbed by the plasma. In addition, because bremsstrahlung rays are not emitted in the opposite direction to that of electron trajectory, intense characteristic X-rays are generated from the plasma-axial direction.

3. Characteristics

3.1. Tube voltage and current

Tube voltage and current were measured by a high-voltage divider with an input impedance of 1 GΩ and a current transformer, respectively. Fig. 3 shows the time relation between the tube voltage and current. At the indicated charging voltages, they roughly displayed damped oscillations. When the charging voltage was increased, both the maximum tube voltage and current increased. At a charging voltage of 50 kV, the maximum tube voltage was almost equal to the charging voltage of the main condenser, and the maximum tube current was approximately 18 kA.

3.2. X-ray output

X-ray output pulse was detected using a combination of a plastic scintillator and a photomultiplier (Fig. 4). The X-ray pulse height substantially increased with corresponding increases in the charging voltage. The X-ray pulse widths were about 300 ns, and the time-integrated X-ray intensity measured by a thermoluminescence dosimeter (Kyokko TLD Reader 1500 having MSO-S elements without energy compensation) had a value of about 1.0 mGy at 1.0 m from the X-ray source with a charging voltage of 50 kV.

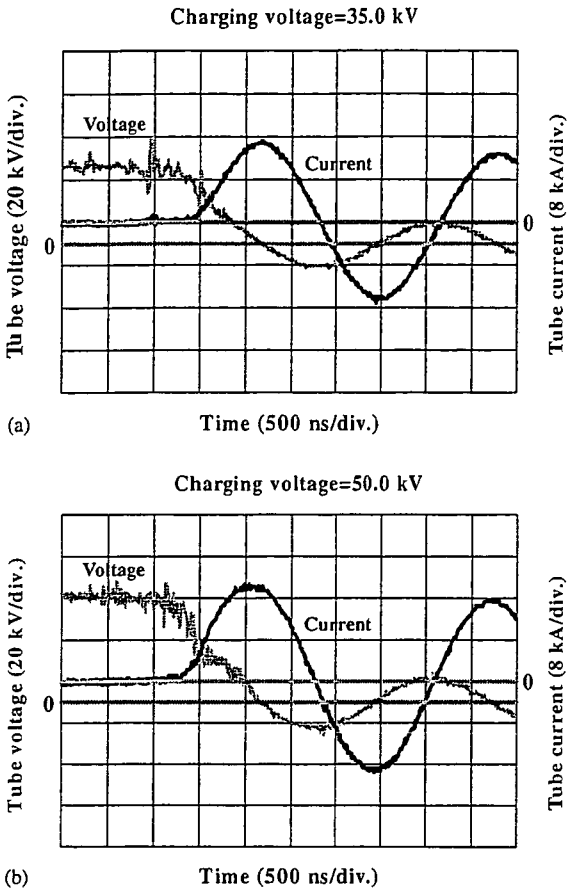

Fig. 3. Tube voltages and currents with a charging voltage of (a) 35.0 kV and (b) 50.0 kV.

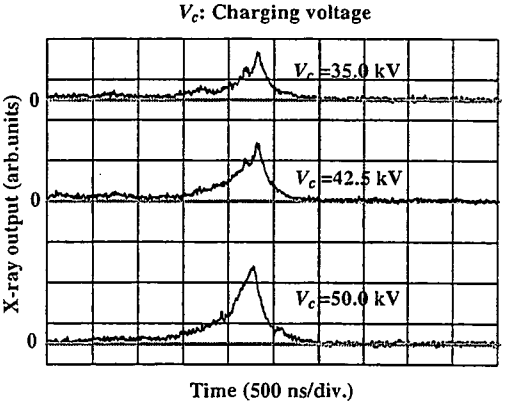

Fig. 4. X-ray outputs at the indicated conditions.

3.3. X-ray source

In order to roughly observe images of the plasma X-ray source in the detector plane, we employed a pinhole camera with a hole diameter of 100 μm (Fig. 5). When

the charging voltage was increased, the plasma X-ray source grew, and both spot dimension and intensity increased. Because the X-ray intensity is the highest at the center of the spot, both the dimension and intensity decreased according to both increases in the thickness of a filter for absorbing X-rays and decreases in the pinhole diameter.

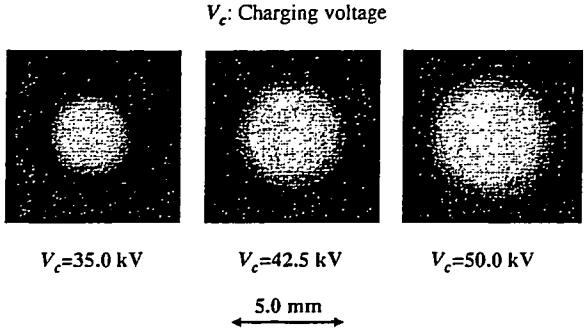

Fig. 5. Images of plasma X-ray source.

3.4. X-ray spectra

X-ray spectra from the plasma source were measured by a transmission-type spectrometer with a lithium fluoride curved crystal 0.5 mm in thickness. The spectra were taken by a computed radiography (CR) system (Sato et al., 2000) (Konica Minolta Regius 150) with a wide dynamic range, and relative X-ray intensity was calculated from Dicom digital data. Subsequently, the relative X-ray intensity as a function of the data was calibrated using a conventional X-ray generator, and we confirmed that the intensity was proportional to the

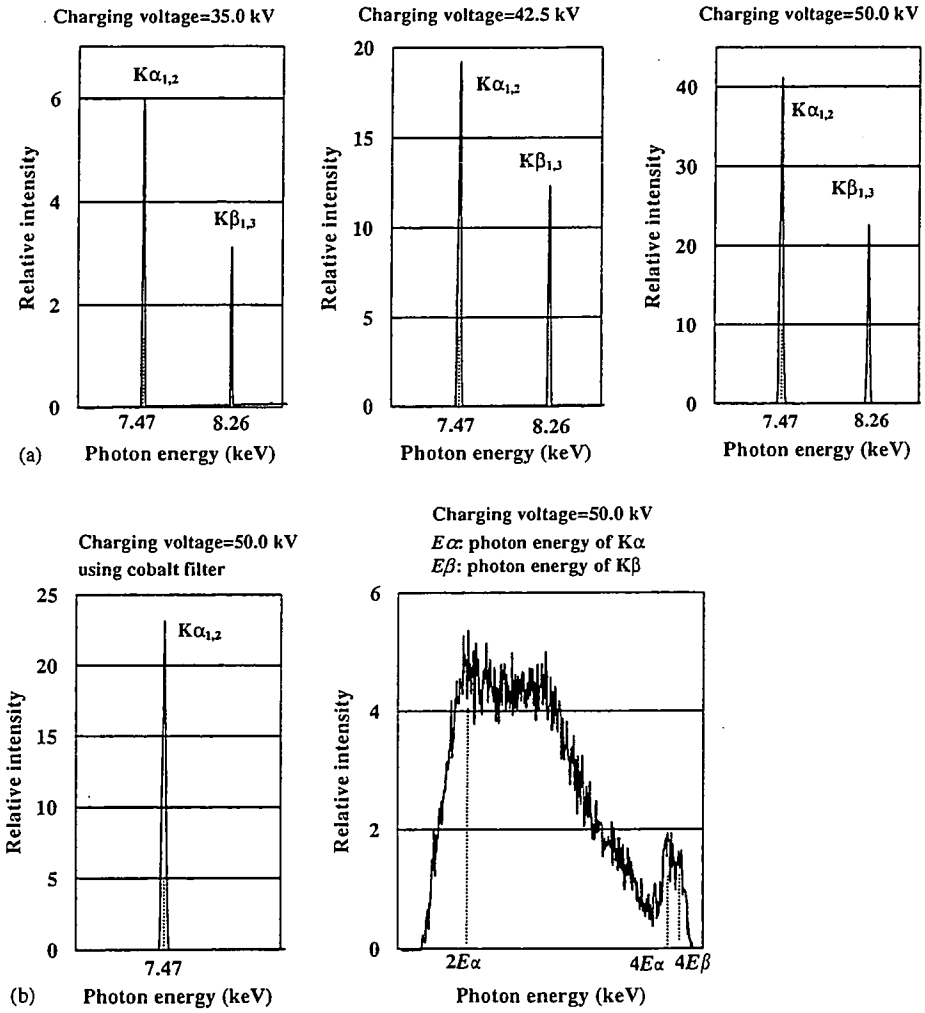

Fig. 6. X-ray spectra from weakly ionized nickel plasma at the indicated conditions. (a) Kα and Kβ rays and (b) Kα and higher harmonic rays.

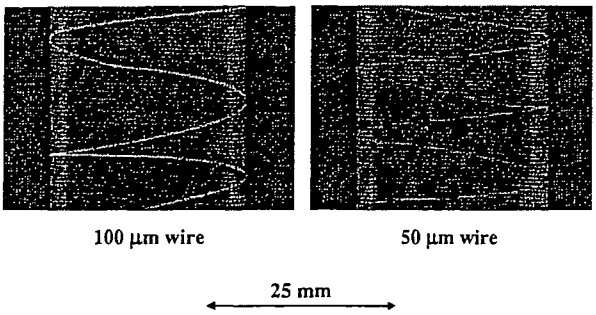

Fig. 7. Radiograms of tungsten wires coiled around PMMA pipes.

exposure time. Fig. 6 shows measured spectra from the copper target with a charging voltage of 50 kV. In fact, we observed clean K lines such as lasers, and Kα lines were left by absorbing Kβ lines using a 15-μm-thick cobalt filter. The characteristic X-ray intensity substantially increased with corresponding increases in the charging voltage, and higher harmonic hard X-rays were observed.

4. Radiography

The plasma radiography was performed by the CR system without using the filter. The charging voltage and the distance between the X-ray source and imaging plate were 50 kV and 1.2 m, respectively.

Firstly, rough measurements of spatial resolution were made using wires. Fig. 7 shows radiograms of tungsten wires coiled around pipes made of polymethyl methacrylate (PMMA). Although the image contrast decreased somewhat with decreases in the wire diameter, due to blurring of the image caused by the sampling pitch of 87.5 μm, a 50-μm-diameter wire could be observed.

Fig. 8 shows a radiogram of a vertebra, and fine structures in the vertebra were observed. Next, an image of plastic bullets falling into a polypropylene beaker from a plastic test tube is shown in Fig. 9. Because the X-ray duration was about 500 ns, the stop-motion image of bullets could be obtained.

5. Conclusions and outlook

Concerning the spectrum measurement, we obtained fairly intense and clean K lines from a weakly ionized linear plasma X-ray source, and Kα lines were left by absorbing Kβ lines using the cobalt filter. In particular, the higher harmonic X-rays were produced from the plasma. Because the X-ray intensities of the harmonics increased with increases in the charging voltage, the

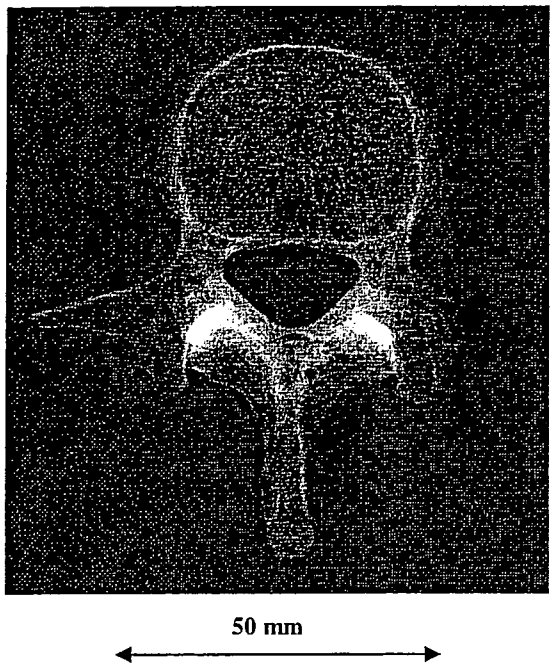

Fig. 8. Radiogram of a vertebra.

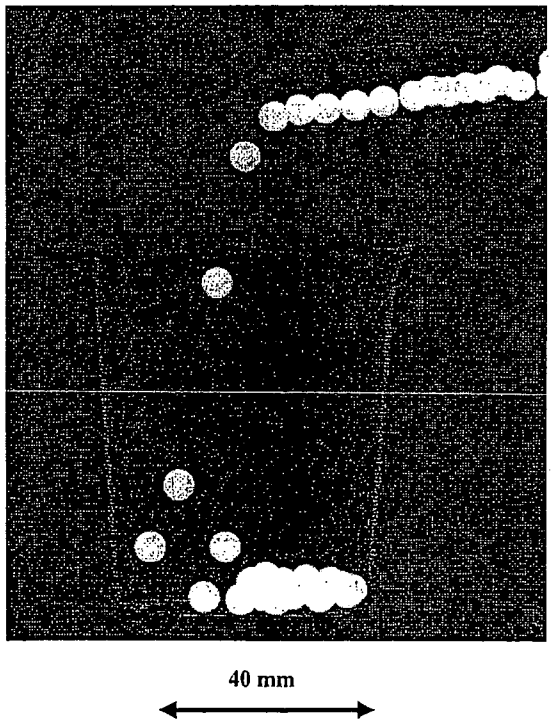

Fig. 9. Radiogram of plastic bullets falling into polypropylene beaker from a plastic test tube.

harmonic bremsstrahlung rays survived due to the X-ray resonation.

To perform monochromatic radiography, the higher harmonics are not necessary. Therefore, the condenser charging voltage should be minimized in order to decrease the intensities of higher harmonics, and the condenser capacity should be maximized to increase the characteristic X-ray intensity. On the other hand, because the intensities of harmonics increase with increases in the charging voltage, high-photon-energy monochromatic radiography may be realized.

In this research, we obtained sufficient characteristic X-ray intensity per pulse for CR radiography, and the generator produced number of characteristic K photons was approximately 1×10^8 photons/cm^2 at 1.0 m per pulse. In addition, since the photon energy of characteristic X-rays can be controlled by changing the target elements, various quasi-monochromatic high-speed radiographies, such as high-contrast angiography and mammography, will be possible.

Acknowledgments

This work was supported by Grants-in-Aid for Scientific Research (13470154, 13877114, 16591181, and 16591222) and Advanced Medical Scientific Research from MECSST, Health and Labor Sciences Research Grants (RAMT-nano-001, RHGTEFB-genome-005 and RHGTEFB-saisei-003), Grants from the Keiryo Research Foundation, the Promotion and Mutual Aid Corporation for Private Schools of Japan, the Japan Science and Technology Agency (JST), and the New Energy and Industrial Technology Development Organization (NEDO, Industrial Technology Research Grant Program in '03).

References

Ando, M., Maksimenko, M., Sugiyama, H., Pattanasiriwisawa, W., Hyodo, K., Uyama, C., 2002. A simple X-ray dark- and bright- field imaging using achromatic Laue optics. Jpn J. Appl. Phys. 41, L1016–L1018.

Davis, T.J., Gao, D., Gureyev, T.E., Stevenson, A.W., Wilkins, S.W., 1995. Phase-contrast imaging of weakly absorbing materials using hard X-rays. Nature 373, 595–597.

Germer, R., 1979. X-ray flash techniques. J. Phys. E: Sci. Instrum. 12, 336–350.

Hyodo, K., Ando, M., Oku, Y., Yamamoto, S., Takeda, T., Itai, Y., Ohtsuka, S., Sugishita, Y., Tada, J., 1998. Development of a two-dimensional imaging system for clinical applications of intravenous coronary angiography using intense synchrotron radiation produced by a multipole wiggler. J. Synchrotron. Rad. 5, 1123–1126.

Macchietto, C.D., Benware, B.R., Rocca, J.J., 1999. Generation of millijoule-level soft-X-ray laser pulses at a 4-Hz repetition rate in a highly saturated tabletop capillary discharge amplifier. Opt. Lett. 24, 1115–1117.

Momose, A., Takeda, T., Itai, Y., Hirano, K., 1996. Phase-contrast X-ray computed tomography for observing biological soft tissues. Nat. Med. 2, 473–475.

Mori, H., Hyodo, K., Tanaka, E., Mohammed, M.U., Yamakawa, A., Shinozaki, Y., Nakazawa, H., Tanaka, Y., Sekka, T., Iwata, Y., Honda, S., Umetani, K., Ueki, H., Yokoyama, T., Tanioka, K., Kubota, M., Hosaka, H., Ishizawa, N., Ando, M., 1996. Small-vessel radiography in situ with monochromatic synchrotoron radiation. Radiology 201, 173–177.

Rocca, J.J., Shlyaptsev, V., Tomasel, F.G., Cortazar, O.D., Hartshorn, D., Chilla, J.L.A., 1994. Demonstration of a discharge pumped table-top soft X-ray laser. Phys. Lev. Lett. 73, 2192–2195.

Rocca, J.J., Clark, D.P., Chilla, J.L.A., Shlyaptsev, V.N., 1996. Energy extraction and achievement of the saturation linit in a discharge-pumped table-top soft X-ray amplifier. Phys. Lev. Lett. 77, 1476–1479.

Sato, E., Kimura, S., Kawasaki, S., Isobe, H., Takahashi, K., Tamakawa, Y., Yanagisawa, T., 1990. Repetitive flash X-ray generator utilizing a simple diode with a new type of energy-selective function. Rev. Sci. Instrum. 61, 2343–2348.

Sato, E., Takahashi, K., Sagae, M., Kimura, S., Oizumi, T., Hayasi, Y., Tamakawa, Y., Yanagisawa, T., 1994a. Sub-kilohertz flash X-ray generator utilizing a glass-enclosed cold-cathode triode. Med. Biol. Eng. Comput. 32, 289–294.

Sato, E., Sagae, M., Takahashi, K., Shikoda, A., Oizumi, T., Hayasi, Y., Tamakawa, Y., Yanagisawa, T., 1994b. 10 kHz microsecond pulsed X-ray generator utilizing a hot-cathode triode with variable durations for biomedical radiography. Med. Biol. Eng. Comput. 32, 295–301.

Sato, E., Sato, K., Tamakawa, Y., 2000. Film-less computed radiography system for high-speed imaging. Ann. Rep. Iwate Med. Univ. Sch. Lib. Arts Sci. 35, 13–23.

Sato, E., Hayasi, Y., Germer, R., Tanaka, E., Mori, H., Kawai, T., Obara, H., Ichimaru, T., Takayama, K., Ido, H., 2003a. Irradiation of intense characteristic X-rays from weakly ionized linear molybdenum plasma. Jpn J. Med. Phys. 23, 123–131.

Sato, E., Hayasi, Y., Germer, R., Tanaka, E., Mori, H., Kawai, T., Ichimaru, T., Takayama, K., Ido, H., 2003b. Quasi-monochromatic flash X-ray generator utilizing weakly ionized linear copper plasma. Rev. Sci. Instrum. 74, 5236–5240.

Sato, E., Sagae, M., Tanaka, E., Hayasi, Y., Germer, R., Mori, H., Kawai, T., Ichimaru, T., Sato, S., Takayama, Y., Ido, H., 2004a. Quasi-monochromatic flash X-ray generator utilizing a disk-cathode molybdenum tube. Jpn J. Appl. Phys. 43, 7324–7328.

Sato, E., Hayasi, Y., Germer, R., Tanaka, E., Mori, H., Kawai, T., Ichimaru, T., Sato, S., Takayama, K., Ido, H., 2004b. Sharp characteristic X-ray irradiation from weakly ionized linear plasma. J. Electron. Spectrosc. Related Phenom. 137–140, 713–720.

Sato, E., Tanaka, E., Mori, H., Kawai, T., Ichimaru, T., Sato, S., Takayama, K., Ido, H., 2004c. Demonstration of

enhanced K-edge angiography using a cerium target X-ray generator. Med. Phys. 31, 3017–3021.

Sato, E., Tanaka, E., Mori, H., Kawai, T., Ichimaru, T., Sato, S., Takayama, Y., Ido, H., 2005a. Compact monochromatic flash X-ray generator utilizing a disk-cathode molybdenum tube. Med. Phys. 32, 49–54.

Sato, E., Tanaka, E., Mori, H., Kawai, T., Sato, S., Takayama, Y., 2005b. High-speed enhanced K-edge angiography utilizing cerium plasma X-ray generator. Opt. Eng. 44, 049001–049016.

Sato, E., Tanaka, E., Mori, H., Kawai, T., Sato, S., Takayama, Y., 2005c. Clean monochromatic X-ray irradiation from weakly ionized linear copper plasma. Opt. Eng. 44, 049002–049016.

Shikoda, A., Sato, E., Sagae, M., Oizumi, T., Tamakawa, Y., Yanagisawa, T., 1994. Repetitive flash X-ray generator having a high-durability diode driven by a two-cable-type line pulser. Rev. Sci. Instrum. 65, 850–856.

Takahashi, K., Sato, E., Sagae, M., Oizumi, T., Tamakawa, Y., Yanagisawa, T., 1994. Fundamental study on a long-duration flash X-ray generator with a surface-discharge triode. Jpn J. Appl. Phys. 33, 4146–4151.

Thompson, A.C., Zeman, H.D., Brown, G.S., Morrison, J., Reiser, P., Padmanabahn, V., Ong, L., Green, S., Giacomini, J., Gordon, H., Rubenstein, E., 1992. First operation of the medical research facility at the NSLS for coronary angiography. Rev. Sci. Instrum. 63, 625–628.

Acta Physiol 2006, 186, 309–318

Does central nitric oxide chronically modulate the acute hypoxic ventilatory response in conscious rats?

D. O. Schwenke,[1] J. T. Pearson,[2] K. Kangawa[1] and M. Shirai[3]

1 *Department of Biochemistry, National Cardiovascular Center Research Institute, Suita, Osaka, Japan*

2 *Department of Physiology, Monash University, Melbourne, Australia*

3 *Faculty of Health Sciences, Hiroshima International University, Hiroshima, Japan*

Received 2 November 2005,
revision requested 28 December 2005,
final revision received 17 February 2006,
accepted 20 February 2006
Correspondence:
D. O. Schwenke, Department of Biochemistry, National Cardiovascular Center Research Institute, 5-7-1 Fujishirodai, Suita, Osaka 565-8565, Japan.
E-mail: schwenke@ri.ncvc.go.jp

Abstract

Aim: Hypoxia initiates an increase in ventilation (V_E) through a cascade of events of which central nitric oxide (NO) has been implicated as an important neuromodulator. There have not been any reports describing the consequences of long-term imbalances in the central NO pathways on the modulation of the acute hypoxic ventilatory response (HVR). Chronic hypoxia (CH) can potentially modify the HVR, and so we hypothesized that central NO may be involved. In this study we describe the long-term role of central NO in the modulation of HVR before and after CH.

Methods: Male Sprague–Dawley rats (BW *c.* 200–320 g; $n = 21$) were implanted with an osmotic pump for continuous intracerebroventricular administration of either artificial cerebrospinal fluid (control), N^{ω}-nitro-L-arginine methyl ester (L-NAME) (150 $\mu g\ kg^{-1}\ day^{-1}$) or the NO-donor, 3-[4-morpholinyl]-sydnonimine-hydrochloride (SIN-1) (100 $\mu g\ kg^{-1}\ day^{-1}$). The V_E response to acute poikilocapnic hypoxia (8% O_2 for 20 min) was measured by plethysmography seven days after surgery, in normoxia, and again after 14 days of exposure to CH (CH = 12% O_2).

Results: The magnitude of the HVR (*c.* 230% increase in V_E) was unaltered by centrally infusing either L-NAME or SIN-1 for 1 week. CH did not modify the HVR, although baseline V_E and HVR were shifted downward by L-NAME during CH – because of a reduction in the frequency component.

Conclusions: These results suggest that long-term alterations in central NO levels may not alter the HVR under moderate CH, presumably because of the onset/development of compensatory mechanisms. However, NO appears to be an important component of the HVR following CH.

Keywords central nervous system, chronic hypoxia, hypoxic ventilatory response, nitric oxide.

Systemic hypoxia initiates a cascade of discrete neural pathways that ultimately leads to a reflex increase in pulmonary ventilation (V_E). Ever since its discovery, nitric oxide (NO) has been implicated in a diverse range of physiological functions. Several studies have implicated NO as an important neuromodulator involved in the ventilatory response to hypoxia (HVR), at both a peripheral and central level.

Nitric oxide is produced from L-arginine in a reaction catalysed by isoenzymes of NO synthase (NOS). The synthesis of NO is blocked by several L-arginine analogues, including N^{ω}-nitro-L-arginine methyl ester (L-NAME), which competitively and stereoselectively inhibits the generation of NO from L-arginine (Palmer *et al.* 1988). NOS has been localized within the nerve fibres innervating the glomus tissue of the carotid bodies

 doi: 10.1111/j.1748-1716.2006.01570.x

– the primary peripheral chemoreceptors (Prabhakar *et al.* 1993, Wang *et al.* 1993). Furthermore, systemic administration of NOS blockers enhances the HVR indicating NO acts as inhibitory neuromodulator at the site of the carotid bodies (Prabhakar *et al.* 1993, Wang *et al.* 1994, Kline *et al.* 1998).

In contrast, NO has been described as an excitatory neuromodulator within the central regions of the brain stem associated with the control of breathing. The enzyme NOS has been localized within the nucleus tractus solitarius (NTS) (Ohta *et al.* 1993, Haxhiu *et al.* 1995), the rostral ventrolateral medulla (Shapoval *et al.* 1991, Kishi *et al.* 2002) the nucleus raphe magnus (Leger *et al.* 1998) and implicated within the locus coeruleus (Fabris *et al.* 2000), and acute inhibition of NOS within these regions attenuates the HVR (Haxhiu *et al.* 1995, de Paula & Branco 2003, Nucci *et al.* 2004). Despite several studies describing the effect of acute NOS inhibition on the HVR, there have not been any reports describing the physiological significance of central NO in the long-term control of breathing, especially with regard to the modulation of HVR. Therefore, we aimed to investigate modulation of the HVR following long-term changes in central NO levels.

Chronic hypoxia (CH) has been reported to modify the HVR, with several studies describing an enhanced HVR (Aaron & Powell 1993, Reinhart *et al.* 1997, Reid & Powell 2005). Dwinell & Powell (1999) suggested that, as carotid body afferents terminate within the NTS (Spyer 1994), CH may enhance the HVR by sensitizing the brainstem to acute hypoxia, so that the integrated afferent signal from the carotid body would be amplified within the NTS and thus enhance ventilatory output.

The precise neuromodulator pathways by which CH enhances the HVR are still not fully understood. Ogawa *et al.* (1995) indicated that microinjections of NO into the NTS enhanced the HVR by amplifying the afferent signal received from the carotid bodies. Therefore, we hypothesized that central NO, which has been shown to enhance NTS neurone excitability and discharge rate (Tagawa *et al.* 1994), may also have a significant role in modifying the HVR following CH in conscious rats.

Materials and methods

Animals

Experiments were conducted on 21 male Sprague–Dawley rats (8 weeks old; BW *c.* 200–320 g). Rats were divided into three groups; Group 1 – control, Group 2 – L-NAME and Group 3 – 3-[4-morpholinyl]-sydnonimine-hydrochloride (SIN-1). All rats were on a 12-h light/dark cycle at 25 ± 1 °C and were provided with food and water *ad libitum*. All experiments were approved by the local Animal Ethics Committee and conducted in accordance with the guidelines of the Physiological Society of Japan.

After surgical implantation of an osmotic pump, all rats were housed in standard normoxic conditions for 1 week and then continuously housed in a hypoxic chamber (12 ± 0.1% O_2) for 2 weeks, except for a 10-min interval each day when the chamber was cleaned. The hypoxic gas mixture was prepared from N_2 (gas cylinders) and compressed air and was continuously delivered to the hypoxic chamber (30 L capacity) at a flow rate of ~8 L min^{-1}.

Anaesthesia and surgical preparation

All surgical procedures were performed using standard aseptic techniques. Rats were anaesthetized with pentobarbital sodium (50 mg kg^{-1}, i.p.). Supplementary doses of anaesthetic (*c.* 15 mg kg^{-1} h^{-1} i.p.) were administered if a limb withdrawal reflex was elicited in response to pinching of a hind footpad. Throughout the surgery body temperature was maintained at 38 °C using a rectal thermistor coupled with a thermostatically controlled heating pad.

Intracerebroventricular catheterization and osmotic pump implantation

Rats were placed on a stereotaxic frame and a skin incision was made along the midline of the skull. A small hole was drilled through the appropriate position on the skull. A 27-gauge stainless steel cannula was positioned in the right lateral cerebral ventricle according to the coordinates of Paxinos & Watson (0.8 mm posterior to the bregma, 1.5 mm lateral to the midline and 5.0 mm ventral to the skull surface) and fixed to the skull with cyanoacrylate adhesive. Correct positioning of the intracerebroventricular (i.c.v.) catheter was confirmed at post-mortem by staining with Evans blue dye (10 μL). If the cerebroventricular surface did not stain, all data from that animal were excluded from analyses.

The distal end of the stainless steel cannula was connected to a miniosmotic pump (Alzet, type 2004; Durect Corporation, Cupertino, CA, USA) via polyethylene tubing (PE 10, I.D. 0.28 mm; OD 0.61 mm). The osmotic pump was inserted through the initial skin incision and tunnelled subcutaneously to the interscapular region. The skin incision was then closed with sutures. The osmotic pump had an infusion rate and duration of 0.25 μL h^{-1} and 4 weeks, respectively. Rats were assigned an osmotic pump filled with either artificial cerebrospinal fluid (aCSF, control), the NO synthase inhibitor L-NAME (150 μg kg^{-1} day^{-1}; Sigma, St Louis, MO, USA), or the slow releasing NO donor, SIN-1 (100 μg kg^{-1} day^{-1}; Tocris Cookson, Avon-

  doi: 10.1111/j.1748-1716.2006.01570.x

mouth, UK). aCSF, which was used as the vehicle for centrally administering drugs, had a pH of 7.36–7.43 and was prepared using 150 mM NaCl, 3.0 mM KCl, 0.8 mM $MgCl_2$, 1.4 mM $CaCl_2$ and 1.0 mM sodium phosphate.

Immediately following surgery, all animals received 30 mg kg^{-1} (i.m.) of Viccillin® antibiotic (Meiji Seika Kaisha, Ltd, Tokyo, Japan) and remained on the heating blanket during recovery from anaesthesia. Rats had 7 days to recover from surgery before data were collected. During this period the welfare of the rat was monitored by recording body weight, food and water consumption, observing general appearance and behaviour, and cleaning and dressing wounds if required.

Measurement of respiratory variables

The barometric method of plethysmography (Bartlett & Tenney 1970) was used to measure tidal volume (V_T). Each rat was placed inside an air-tight Perspex chamber (within a restrainer to prevent backward rotation) which was incorporated in a unidirectional flow circuit into which either normoxia or hypoxia was delivered. Gases flowing into the chamber (*c.* 2 L min^{-1}) were first humidified (100% saturation) and the chamber was heated (27–29 °C) to ensure that, first, rats were within their thermoneutral zone and, secondly, rats were warmed to ensure adequate blood flow to the tail; an essential requisite for measuring ABP via the tail-cuff method (Bunag 1973) – see below. Each time V_T was to be measured, the flow of gas into and out of the chamber was temporarily interrupted by sealing the inlet and outlet gas ports for *c.* 30 s, and the changes in chamber pressure associated with inspiration and expiration were recorded. For each V_T measurement, chamber temperature and body temperature were measured (to one decimal place) with a Fluke thermocouple thermometer (model 52II, Fluke Co., Everett, WA, USA). Barometric pressure was recorded on each day of an experiment. Calibration for volume was achieved by injecting a known set volume (0.2 mL) into the chamber at a rate similar to that of a rat.

The acute poikilocapnic hypoxic test gas (i.e. $8 \pm 0.2\%$ O_2) was created using O_2 and N_2 gas rotameters and verified using a Sable oxygen analyzer (FC-2 Oxygen Analyzer; Sable Systems, Henderson, NV, USA). When the inlet gas composition was changed, *c.* 2 min was required for the chamber to be fully flushed with the new gas.

Measurement of arterial blood pressure

Systolic and diastolic blood pressures and heart rate were recorded in conscious animals using an automatic sphygmomanometer tail cuff pressure transducer (BP-98A; Softron Co. Ltd, Tokyo, Japan). Each value recorded was derived from five consecutive measurements (within approximately 4 min), which were then averaged to give one mean value representative of each experimental condition. Mean arterial blood pressure (MABP) was calculated from systolic and diastolic pressures.

Experimental protocol

Training. All rats were subjected to the acute hypoxic protocol in the conscious state. However, each rat was first trained to sit restfully within a Perspex chamber (*c.* 2.5 L) to avoid stress or anxiety influencing the results. Training started 4 days after surgery and was achieved by exposing each rat to air for 60 min (day 1 & 2 of training) or the acute hypoxic protocol (day 3 of training). By the fourth day (i.e. 1 week post-surgery), rats were considered trained and ventilatory data were collected from conscious rats during normoxia and in response to acute hypoxia. Additionally, rats were re-familiarized with the protocol by being placed in a chamber after 1 week of CH.

Acute hypoxic protocol. Ventilatory responses to poikilocapnic hypoxia (20 min of 8% O_2) were tested in all rats after 1 week of normoxia, and then again after 2 weeks of CH (12% O_2). On the day of an experiment, each rat was initially placed inside the Perspex chamber and allowed 30 min to become accustomed, after which data collection began. Rats were first subjected to measurements under normoxia for 10 min before being exposed to acute hypoxia (8% O_2 in N_2) for 20 min.

Data acquisition and analysis

The signal corresponding to plethysmograph pressure fluctuations (i.e. tidal volume – V_T) was detected by a SenSym flow pressure transducer (TRD 5100; Buxco Electronics Inc., Sharon, CT, USA), and amplified using a strain gauge preamplifier (Buxco Electronics Inc.). The signal was then sampled at 200 Hz with an 8-channel MacLab/8s interface hardware system (AD Instruments Ltd, Tokyo, Japan) and recorded on a Macintosh Power Book G4 using CHART (v. 5.0.1; AD Instruments). Breathing frequency (freq) was derived from the V_T peaks. Minute ventilation (V_E) was calculated off-line as the product of V_T and frequency and normalized to 100 g BW (BTPS).

A 30-s block of data was analysed −10, −5 min and immediately before (time '0') acute hypoxic exposure and then after 1, 2, 4, 6, 10, 15 and 20 min of exposure to 8% O_2. Normoxic baseline data for individual rats in each group were averaged from values acquired at −5, −10 min and time 0. ABP and HR measurement procedures were carried out once during normoxia

 doi: 10.1111/j.1748-1716.2006.01570.x

and then again between the 10th and 15th minute of acute hypoxia. The MABP and HR values for air and hypoxia were entered into spreadsheets for further statistical analysis.

Statistical analysis

All statistical analyses were conducted using STATVIEW (v5.01; SAS Institute, Cary, NC, USA). All results are presented as mean ± standard error of the mean (SEM). Two-way ANOVA (repeated measures) was used to test significance for (i) temporal changes in each variable in response to 20 min of acute hypoxia and (ii) alterations in the hypoxic response by central drug administration or CH. One-way ANOVA (factorial) was used to test the differences in the baseline values for normoxia compared with CH. Where statistical significance was reached, *post hoc* analyses were incorporated using the paired, or unpaired *t*-test with the Dunnet's correction for multiple comparisons. A *P*-value ≤0.05 was predetermined as the level of significance for all statistical analysis.

Results

Baseline

Baseline data were collected from rats in normoxia 1 week after receiving a continuous i.c.v. infusion of either aCSF (control, $n = 6$), L-NAME ($n = 8$) or SIN-1 ($n = 7$). The data are presented in Table 1. There were no significant differences in any of the cardioventilatory baseline variables between all three groups of rats. However, the rats that received a central infusion of SIN-1 had a slightly, albeit significant ($P = 0.002$), higher T_B (39.0 ± 0.2 °C), than the control rats (38.1 ± 0.1 °C).

Two weeks of CH provoked an 18% increase in V_E (NS) in control rats due to a 22% increase in V_T ($P = 0.03$). Rats treated with SIN-1 were not significantly different to control rats. In contrast, in rats treated with L-NAME, CH caused a significant 13% decrease in V_E primarily due to a 24% decrease in respiratory frequency ($P = 0.003$). In all three groups of rats, CH did not significantly change T_B, MABP or HR (Table 1).

Responses to acute hypoxia

In control normoxic rats, acute exposure to 8% O_2 provoked an increase in V_E, significant by the second minute, reaching a plateau by the sixth minute, and remaining *c.* 230% above baseline values until the end of hypoxic exposure (Fig. 1). The HVR response comprised freq (*c.* 105%) and even larger V_T (*c.* 140%) responses. The magnitude and pattern of the HVR for L-NAME rats was similar to that of control rats (Fig. 1). Rats treated with SIN-1 also had a

Table 1 Baseline cardio-ventilatory data of conscious rats in normoxia and after 2 weeks of chronic hypoxia (CH – 12% O_2)

	Control	L-NAME	SIN-1
Pre-CH			
Body weight (g)	236 (218–252)	231 (198–270)	263 (198–320)
V_E (mL min^{-1} 100 g^{-1})	76.2 ± 7.6	75.3 ± 2.9	82.8 ± 4.7
V_T (mL 100 g^{-1})	0.48 ± 0.03	0.47 ± 0.02	0.56 ± 0.05
Freq (b min^{-1})	158 ± 10	161 ± 10	152 ± 13
T_b (°C)	38.13 ± 0.11	38.54 ± 0.13†	39.04 ± 0.18†
HR (b min^{-1})	386 ± 19	404 ± 25	388 ± 10
MABP (mmHg)	87 ± 5	94 ± 7	98 ± 4
CH (12% O_2 for 2 weeks)			
Body weight (g)	271	(262–302)	277
V_E (mL min^{-1} 100 g^{-1})	89.7 ± 8.8	65.5 ± 3.2*,†	86.4 ± 7.1
V_T (mL 100 g^{-1})	0.59 ± 0.03*	0.54 ± 0.04	0.63 ± 0.03
Freq (b min^{-1})	152 ± 13	121 ± 2**,†	138 ± 13
T_b (°C)	38.43 ± 0.17	38.30 ± 0.14	38.74 ± 0.27
HR (b min^{-1})	412 ± 9	390 ± 17	365 ± 6**
MABP (mmHg)	96 ± 3	98 ± 3	111 ± 6

Data are presented as mean ± SEM (except for body weight which presents the range in parentheses). Data were collected from rats that had a continuous infusion of either artificial cerebrospinal fluid (i.e. control, $n = 6$), N^{ω}-nitro-L-arginine methyl ester (L-NAME) (150 μg kg^{-1} day^{-1}; $n = 8$) or 3-[4-morpholinyl]-sydnonimine-hydrochloride (SIN-1) (100 μg kg^{-1} day^{-1}; $n = 7$).
Significantly different from normoxia values ($P < 0.05$; **$P < 0.01$).
†Significantly different from 'Control' values ($P < 0.05$).

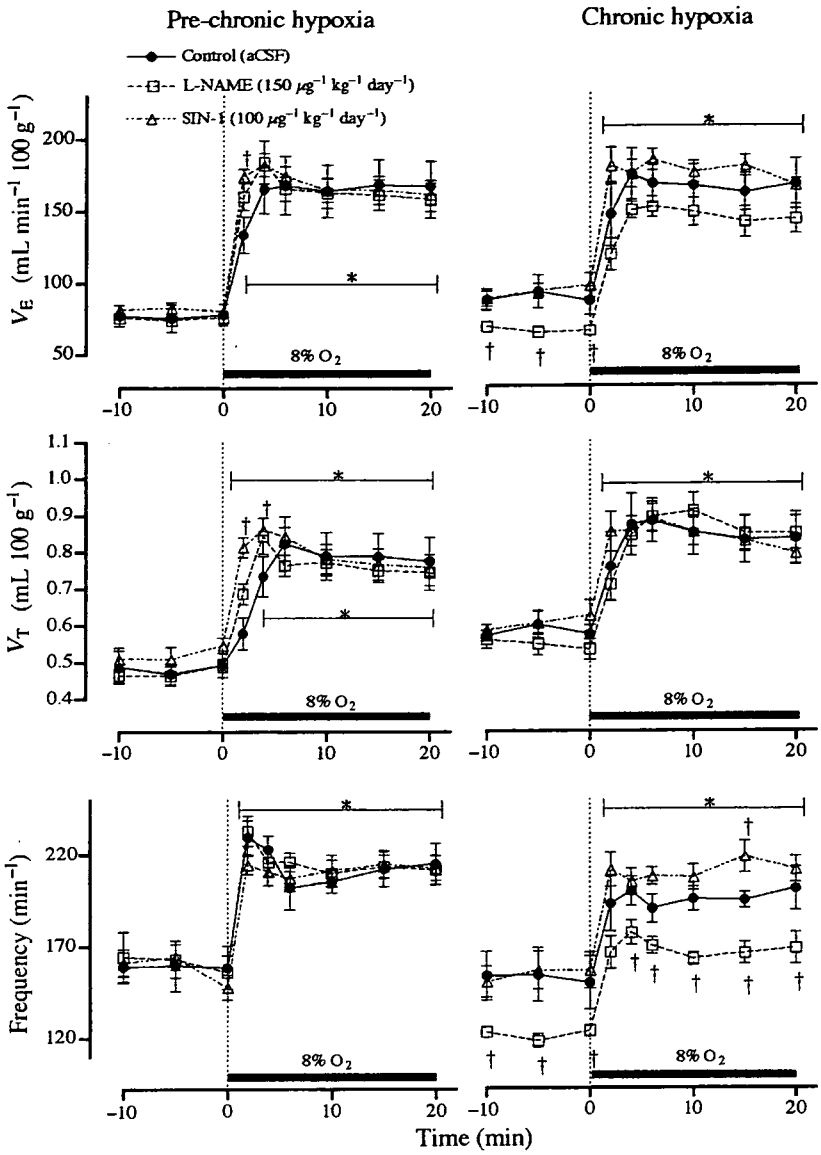

Figure 1 Transient ventilatory (V_E), tidal volume (V_T) and respiratory frequency responses to acute hypoxia (8% O_2 for 20 min) in rats that received a continuous intracerebroventricular infusion of either artificial cerebrospinal fluid (control, $n = 6$ – closed circles), N^{ω}-nitro-L-arginine methyl ester (150 μg kg^{-1} day^{-1}, $n = 8$ – open squares) or 3-[4-morpholinyl]-sydnonimine-hydrochloride (100 μg kg^{-1} day^{-1}, $n = 7$ – open diamonds). Measurements were made prior to and after 2 weeks of chronic hypoxia (12% O_2). †Significantly different from 'control' values ($P < 0.05$). *Significantly different from normoxia (immediately prior to acute hypoxia) values ($P < 0.05$).

similar steady-state HVR from the sixth minute of hypoxia. However, the initial V_E response to acute hypoxia (within 4 min) was significantly more robust in SIN-1 rats compared with that of control rats, because of a more rapid increase in V_T (Fig. 1). Acute hypoxia consistently provoked an increase in HR in all three groups of rats (*c.* 35% increase – Fig. 2), but did not significantly affect MABP. Acute hypoxia caused a significant decrease in T_B after 20 min in control rats only (Fig. 2).

The magnitude and pattern of the HVR was not significantly altered after 2 weeks of CH in control rats or SIN-1-treated rats (Fig. 1). Although CH did not significantly alter the magnitude of the HVR in L-NAME-treated rats, the transient frequency response, and to some degree the V_E response, was shifted downward ($P < 0.05$) (Fig. 1). Neither drug altered the V_T response to acute hypoxia. In general, CH attenuated the HR response to acute hypoxia in all three groups of rats, and did not significantly alter MABP or T_B (Fig. 2).

 doi: 10.1111/j.1748-1716.2006.01570.x

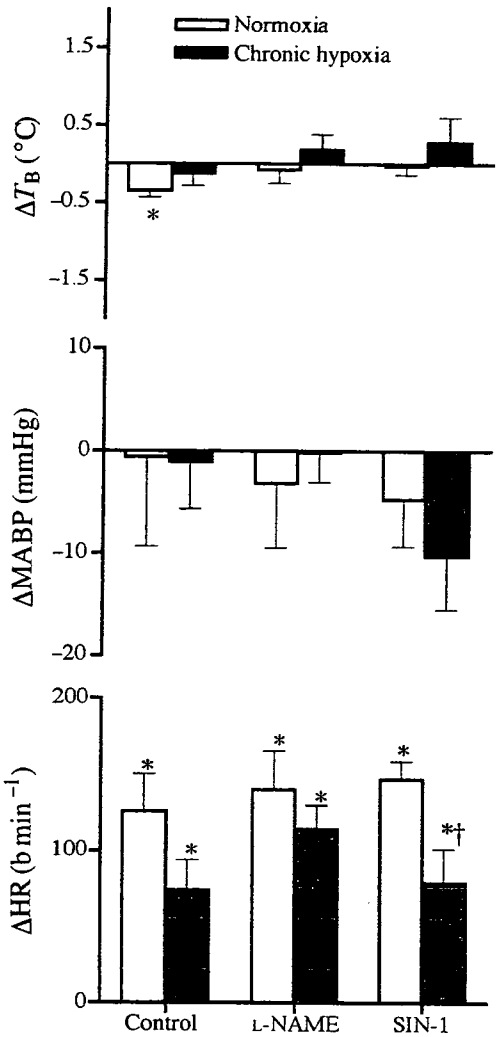

Figure 2 Changes in body temperature (T_B), mean arterial blood pressure (MABP) and heart rate (HR) during exposure to acute hypoxia (8% O_2 for 20 min) in rats that received a continuous intracerebroventricular infusion of artificial cerebrospinal fluid (control, $n = 6$), N^{ω}-nitro-L-arginine methyl ester (150 μg kg^{-1} day^{-1}, $n = 8$) or 3-[4-morpholinyl]-sydnonimine-hydrochloride (100 μg kg^{-1} day^{-1}, $n = 7$). Acute hypoxia measurements were made prior to chronic hypoxia (normoxia = open bars) and after 2 weeks of exposure to 12% O_2 (chronic hypoxia = grey bars). *Significant response to acute hypoxia ($P < 0.05$). †Significant difference in the acute hypoxic response during 'normoxia' and after 'chronic hypoxia' treatment ($P < 0.05$).

Discussion

The primary findings of this study are (i) that chronic alterations in central NO pathways do not appear to alter baseline V_E or the acute HVR in normoxic rats, however (ii) chronic central NOS inhibition appears to reduce both baseline V_E and the peak V_E response to acute hypoxia after 2 weeks of CH. These results highlight the importance of central NO in modulation the HVR after CH.

This is the first study to describe the consequences of chronic disruption in central NO pathways in modulating the HVR. Haxhiu *et al.* (1995) reported that daily intraperitoneal injections of L-NAME for 7 days (150 mg day^{-1}) attenuated the HVR in rats. They concluded that an observed reduction in central cGMP (an index of NO production) was evidence that the attenuated HVR was because of the chronic central inhibition of NO. However, as the L-NAME was administered peripherally at high doses, it is likely that NOS inhibition also occurred within the carotid bodies, which could potentially make it difficult to clearly discriminate between central and peripheral components contributing to the HVR.

Kline *et al.* (1998) reported that NOS-1 knock-out mice had an exaggerated HVR (compared with wild-type mice) and concluded that NO had an inhibitory effect on the HVR, not only at the site of the carotid bodies, but also centrally within the brainstem (comparing cGMP levels). The latter conclusion is in contrast to numerous other reports in the literature indicating that NO acts as an excitatory neuromodulator within the brainstem with regard to the HVR (Ogawa *et al.* 1995, Nakano *et al.* 2001, Nucci *et al.* 2004). In a subsequent report, Kline & Prabhakar (2000) noted that NOS-1 and NOS-3 knock-out mice had an accentuated and attenuated HVR, respectively, compared with wild-type mice. They concluded that NO has a diverse effect on the control of breathing due to the various isoforms of NOS. Although the use of NOS knock-out mice provides invaluable data concerning the global role of NO in the control of breathing, it can potentially be difficult to specifically discriminate between central and peripheral components contributing to the HVR.

Given the numerous reports in the literature indicating that acute central NO inhibition attenuates the HVR, we were surprised that prolonged alterations in central NOS levels did not modify the overall magnitude of the HVR in conscious rats. The precise reason(s) for this observation is uncertain. In this study, it was essential to use a sufficient dose of each drug that would selectively alter central NO levels without having any direct peripheral effect – NO is a lipophilic molecule and L-NAME can cross the blood–brain barrier (Bansinath *et al.* 1993). Therefore, we used doses of L-NAME (150 μg kg^{-1} day^{-1}) and SIN-1 (100 μg kg^{-1} day^{-1}) that did not have any systemic effect when directly administered intravenously. In doing so, we were confident that NO was not acting peripherally to directly attenuate carotid body sensory discharge (Prabhakar *et al.* 1993) which would antagonize the central effects of NO (or NOS inhibition) on the HVR (Gozal *et al.* 1996).

 doi: 10.1111/j.1748-1716.2006.01570.x

It is unlikely that the selected dose of L-NAME (150 $\mu g\ kg^{-1}\ day^{-1}$) was insufficient to cause central NOS inhibition, as Qadri *et al.* (1999) reported that an L-NAME dose of 50 $\mu g\ kg^{-1}\ day^{-1}$ (i.c.v.) for 1 week was sufficient to significantly reduce central NOS activity. Their group, which investigated the role of central NO on the control of MABP, subsequently described that NOS inhibition caused a mild, but significant, increase in MABP (118–125 mmHg). In this study, even though we used a higher chronic dose of L-NAME than that of Qadri *et al.* (1999), we did not observe a significant increase in MABP in conscious rats. Similarly, Wada *et al.* (1998) reported that, despite a significant reduction in brain NO synthesis, MABP was not altered after 1 week of centrally infusing the NOS antagonist, N^G-monomethl-L-arginine (L-NMMA). They reasoned that the lack of MABP response may be attributed to counter-regulatory mechanisms within the CNS acting against NOS inhibition. In the same way, it is reasonable to speculate that in our study prolonged central NOS inhibition did not alter the HVR in a normal, healthy rat in a normoxic environment because other physiological mechanisms are likely to compensate in order to maintain homeostatic control of baseline ventilation and HVR. For example, the non-specific NOS inhibitor L-NAME is known to reduce brain blood flow (Buchanan & Phillis 1993), which can potentially elicit an increase in V_E (Chapman *et al.* 1979). Such an effect could potentially offset, at least to some degree, the direct inhibitory neuronal effects of L-NAME within the respiratory control centres.

One limitation of this study is the absence of immuno-histochemical or biochemical analyses to assess relative changes in NOS expression within the CNS. As mentioned above central NO inhibition has been reported to reduce NOS activity (Qadri *et al.* 1999) and NO synthesis (Wada *et al.* 1998). However, Haxhiu *et al.* (1995) noted that chronic L-NAME treatment (daily i.p. injections) in rats provoked an upregulation in the expression of NOS within the NTS. Collectively, these reports may suggest that a reduction in NO production acts as a stimulus for upregulating NOS expression within the central respiratory centres. This is indeed an area that warrants further research.

Repeated exposure to short bouts of hypoxia can potentially alter the plasticity of the HVR, i.e. Long-Term Facilitation (for a detailed review on LTF, see Mitchell & Johnson 2003). In this study, although unlikely, exposure to acute hypoxia during 'training' (on day 6 post-operative, see 'Methods') may have modified the HVR that was recorded on day 7. However, as the 'training' and 'experimental' hypoxic protocols were similar for all groups of rats, it is unlikely that LTF would have been a significant variable between the different groups of rats.

Another possible reason as to why chronic alterations in central NO did not alter the HVR relates to the diverse effects of central NO. In our study, L-NAME and SIN-1 were infused i.c.v. so that there was a generalized effect of each drug throughout the brainstem rather than a precisely localized effect. Within the regions of the brainstem associated with ventilatory control, NO can mediate both inhibitory and excitatory components of the HVR (Nucci *et al.* 2004). NO has an excitatory action within the NTS (Tagawa *et al.* 1994, Ogawa *et al.* 1995) and rostroventrolateral medulla (RVLM) (de Paula & Branco 2003), although it exerts an inhibitory effect within the regions of the locus coeruleus (Fabris *et al.* 2000) and nucleus raphe magnus (Nucci *et al.* 2004). However, as the later two regions are inhibitory nuclei (Fabris *et al.* 2000, Gargaglioni *et al.* 2003), NO effectively attenuates the inhibitory influence of these two nuclei during hypoxia, thereby enhancing the HVR (Fabris *et al.* 2000, Nucci *et al.* 2004).

Ogawa *et al.* (1995) reported that, within the NTS, the NO-donor sodium nitroprusside (SNP – 10 nmol) enhanced the HVR, concluding that NO has an excitatory role within the NTS. In stark contrast, Vitagliano *et al.* (1996) reported that injecting the NO-donors SNP (40–200 mmol) and SIN-1 (20–100 mmol) into the NTS induced apnoea and concluded that NO within the NTS had an inhibitory effect. Although the discrepancies between studies may be attributed, at least in part, to the high doses of SNP (compared with Ogawa *et al.*) and SIN-1 (compared with our study) used by Vitagliano *et al.* (1996) (which could potentially have a direct peripheral effect), it may also be possible that such discrepancies are partially attributed to the diverse central actions of NO.

One further limitation of this study is that we did not measure metabolism (i.e. oxygen consumption, V_{O_2}). During normoxia, acute NOS blockade reduces V_E, body temperature (T_B) and V_{O_2} (Barros & Branco 2002, Subramanian *et al.* 2002). In our study, the chronic central treatment of L-NAME did not appear to alter baseline V_E. Furthermore, although we did not measure V_{O_2}, it seems unlikely that L-NAME treated rats had a lower basal metabolic rate as T_B was not lower than that of control rats. In fact, we were somewhat surprised that the T_B of rats chronically treated with L-NAME and SIN-1 had a slightly, albeit significant, higher T_B. We are unsure as to the reason for these observations, especially since V_E was similar between all groups of rats.

Exposure to hypoxia causes a decrease in V_{O_2} and T_B, of which both variables are closely correlated. The magnitude of metabolic depression is, to some extent,

 doi: 10.1111/j.1748-1716.2006.01570.x

dependant on ambient temperature. In this study, we aimed to limit the decrease in $\dot{V}O_2$ (and T_B) by recording data from rats that were within their thermoneutral zone (27–29 °C). Gozal *et al.* (1997) did not measure $\dot{V}O_2$ but reasoned that any difference in V_E between control and L-NAME treated rats is unlikely due to a difference in $\dot{V}O_2$ if rats are within their thermoneutral zone. However, in our study, we still noted a small decrease in T_B in control rats during acute hypoxia (pre-CH only) that may be associated with a decrease in $\dot{V}O_2$.

Central NOS inhibition can potentially attenuate the hypoxia-induced decrease in $\dot{V}O_2$ (Gautier & Murariu 1999) and T_B (Branco *et al.* 1997). In our study, although the HVR was not different between groups of rats, we did note that T_B did not decrease during hypoxia in L-NAME treated rats. Whether this observation is solely because of changes in central NO levels is unsure as T_B did not decrease in SIN-1 treated rats. Therefore, as we did not measure metabolism we cannot exclude the possibility that the similar HVR for L-NAME and control rats was matched by different metabolic responses. Furthermore, we are unable to establish whether the lower baseline V_E in L-NAME-treated rats following 2 weeks of CH (discussed below) was associated with a decrease in $\dot{V}O_2$ (T_B was similar between all groups of rats).

The fact that L-NAME or SIN-1 did not alter MABP in the rats of this study may also be explained by the diverse actions of NO within the brainstem. Shapoval *et al.* (1991) demonstrated that central NO inhibition (using L-NMMA) could either increase or decrease MABP, if the NO inhibition was selectively localized to within the RVLM or caudal ventrolateral medulla, respectively. Consequently, it is possible in this study that generalized changes in central NO levels altered the diverse actions of NO within the brain, such that the actual physiological functional responses to hypoxia were unaltered.

In this study we reported that CH did not modify the HVR. According to the literature, CH can potentially attenuate (Wach *et al.* 1989, Mortola 1996), enhance (Aaron & Powell 1993, Dwinell & Powell 1999, Reeves *et al.* 2003) or have no effect on the HVR (Weil 1986), depending on factors such as species, strain, the intensity and duration of CH (Dempsey & Forster 1982) and even intraspecies variation (Aaron & Powell 1993). Although the central mechanisms by which CH modifies the HVR are still not completely understood, Dwinell & Powell (1999) suggested that CH enhanced the responsiveness of the CNS to the afferent input that it receives from the carotid bodies (Powell *et al.* 2000). Furthermore, several studies have implicated alterations in multiple central receptor pathways for enhancing CNS responsiveness, such as those associated with N-methyl-D-aspartate (NMDA) (Ohtake *et al.* 1998, Reeves *et al.* 2003, Reid & Powell 2005), platelet activating factor (Gozal *et al.* 1998), tyrosine hydroxylase (Schmitt *et al.* 1994) and dopamine (Dwinell *et al.* 2000).

This is the first study to investigate the long-term role of NO on the HVR following CH. We found that, although CH did not alter the HVR, it did 'unmask' a potential role of NO in modulating the HVR that had not been apparent prior to CH. Therefore, it is reasonable to speculate that central NO pathways might be, at least partially, involved in increasing CNS sensitivity to carotid body afferent signals following CH. Additionally, although NO may not have been important in the HVR prior to CH (because of potential compensatory mechanisms) it appears to have a significant role in preventing a downward shift of the HVR after CH. This may well be a physiological adaptation or benefit of optimizing cardio-ventilatory control in a 'hostile' environment (Boutilier 2001, Reeves *et al.* 2003).

The structural and biochemical changes in central NO/NOS pathways that may occur during CH are currently unknown. Yet, it has been reported that CH limits endogenous NO synthesis within pulmonary vessels (Sato *et al.* 1999) despite an increase in NOS expression (Shirai *et al.* 2003). Therefore, it remains an essential area of future research to examine central changes in NOS expression following CH.

We have previously reported that 12% O_2 for 2 weeks induces severe pulmonary hypertension and right ventricular hypertrophy (Schwenke *et al.* 2005). Yet a similar CH protocol did not alter the HVR in the present study. It is possible, therefore, that a more severe level of CH (e.g. 10% O_2) may alter the HVR, and if so, we suspect that the role of central NO in maintaining a robust HVR would be even more critical. This is an issue that should be considered in future studies.

In summary, long-term changes in central NO pathways do not appear to have a direct influence on baseline V_E or HVR in normoxic rats, presumably because of homeostatic mechanisms that compensate for the prolonged alterations in central NO. However, NO may have a role, at least in part, in CNS sensitization following CH and, therefore, appears to have an important role in the HVR after CH. Follow-up immunohistochemical/biochemical studies are essential to establish central changes in NOS expression and its relationship to changes in HVR following CH.

Conflict of interest

Concerning the material presented in this manuscript, there are no conflicts of interest.

  doi: 10.1111/j.1748-1716.2006.01570.x

This study was supported in part by the 'Program for Promotion of Fundamental Studies in Health Sciences of the National Institute of Biomedical Innovation (NIBIO)' and also in part by a Grant-in Aid for Scientific Research (no. 16659210).

References

Aaron, E.A. & Powell, F.L. 1993. Effect of chronic hypoxia on hypoxic ventilatory response in awake rats. *J Appl Physiol* 74, 1635–1640.

Bansinath, M., Arbabha, B., Turndorf, H. & Garg, U.C. 1993. Chronic administration of a nitric oxide synthase inhibitor, N-nitro-L-arginine, and drug-induced increase in cerebellar cyclic GMP in vivo. *Neurochem Res* 18, 1063–1066.

Barros, R.C. & Branco, L.G. 2002. Central dopamine modulates anapyrexia but not hyperventilation induced by hypoxia. *J Appl Physiol* 92, 975–981.

Bartlett, D.J.B. & Tenney, S.M. 1970. Control of breathing in experimental anemia. *Resp Physiol* 10, 384–395.

Boutilier, R.G. 2001. Mechanisms of cell survival in hypoxia and hypothermia. *J Exp Biol* 204, 3171–3181.

Branco, L.G., Carnio, E.C. & Barros, R.C. 1997. Role of the nitric oxide pathway in hypoxia-induced hypothermia of rats. *Am J Physiol (Reg Int Comp Physiol)* 273, R967–R971.

Buchanan, J.E. & Phillis, J.W. 1993. The role of nitric oxide in the regulation of cerebral blood flow. *Brain Res* 610, 248–255.

Bunag, R.D. 1973. Validation in awake rats of a tail-cuff method for measuring systolic pressure. *J Appl Physiol* 34, 279–282.

Chapman, R.W., Santiago, T.V. & Edelman, N.H. 1979. Effects of graded reduction of brain blood flow on ventilation in unanesthetized goats. *J Appl Physiol* 47, 104–111.

Dempsey, J.A. & Forster, H.V. 1982. Mediation of ventilatory adaptations. *Physiol Rev* 62, 262–346.

Dwinell, M.R. & Powell, F.L. 1999. Chronic hypoxia enhances the phrenic nerve response to arterial chemoreceptor stimulation in anesthetized rats. *J Appl Physiol* 87, 817–823.

Dwinell, M.R., Huey, K.A. & Powell, F.L. 2000. Chronic hypoxia induces changes in the central nervous system processing of arterial chemoreceptor input. *Adv Exp Med Biol* 475, 477–484.

Fabris, G., Steiner, A.A., Anselmo-Franci, J.A. & Branco, L.G. 2000. Role of nitric oxide in rat locus coeruleus in hypoxia-induced hyperventilation and hypothermia. *Neuroreport* 11, 2991–2995.

Gargaglioni, L.H., Coimbra, N.C. & Branco, L.G. 2003. The nucleus magnus modulates hypoxia-induced hyperventilation but not anapyrexia in rats. *Neurosci Lett* 347, 121–125.

Gautier, H. & Murariu, C. 1999. Role of nitric oxide in hypoxic hypometabolism in rats. *J Appl Physiol* 87, 104–110.

Gozal, D., Torres, J.E., Gozal, Y.M. & Littwin, S.M. 1996. Effect of nitric oxide synthase inhibition on cardiorespiratory responses in the conscious rat. *J Appl Physiol* 81, 2068–2077.

Gozal, D., Gozal, E., Torres, J.E., Gozal, Y.M., Nuckton, T.J. & Hornby, P.J. 1997. Nitric oxide modulates ventilatory responses to hypoxia in the developing rat. *Am J Resp Crit Care Med* 155, 1755–1762.

Gozal, D., Holt, G.A., Graff, G.R. & Torres, J.E. 1998. Platelet-activating factor modulates cardiorespiratory responses in the conscious rat. *Am J Physiol* 275, R604–R611.

Haxhiu, M.A., Chang, C.H., Dreshaj, I.A., Erokwu, B., Prabhakar, N.R. & Cherniack, N.S. 1995. Nitric oxide and ventilatory response to hypoxia. *Resp Physiol* 101, 257–266.

Kishi, T., Hirooka, Y., Ito, K., Sakai, K., Shimokawa, H. & Takeshita, A. 2002. Cardiovascular effects of overexpression of endothelial nitric oxide synthase in the rostral ventrolateral medulla in stroke-prone spontaneously hypertensive rats. *Hypertension* 39, 264–268.

Kline, D.D. & Prabhakar, N.R. 2000. Peripheral chemosensitivity in mutant mice deficient in nitric oxide synthase. *Adv Exp Med Biol* 475, 571–579.

Kline, D.D., Yang, T., Huang, P.L. & Prabhakar, N.R. 1998. Altered respiratory responses to hypoxia in mutant mice deficient in neuronal nitric oxide synthase. *J Physiol* 511, 273–287.

Leger, L., Gay, S., Burlet, Y., Charnay, R. & Cespuglio, R. 1998. Localization of nitric oxide-synthesizing neurons sending projections to the dorsal raphe nucleus of the rat. *Neurosci Lett* 257, 147–150.

Mitchell, G.S. & Johnson, S.M. 2003. Neuroplasticity in respiratory motor control. *J Appl Physiol* 94, 358–374.

Mortola, J.P. 1996. Ventilatory responses to hypoxia in mammals. In: G.G. Hadda & G. Lister (eds) *Tissue Oxygen Deprivation: Developmental Molecular and Integrated Function*, pp. 433–477. Dekker, New York.

Nakano, H., Lee, S.D., Ray, A.D., Krasney, J.A. & Farkas, G.A. 2001. Role of nitric oxide in thermoregulation and hypoxic ventilatory response in obese Zucker rats. *Am J Resp Crit Care Med* 164, 437–442.

Nucci, T.B., Branco, L.G. & Gargaglioni, L.H. 2004. Nitric oxide pathway in the nucleus raphe magnus modulates hypoxic ventilatory response but not anapyrexia in rats. *Brain Res* 1017, 39–45.

Ogawa, H., Mizusawa, A., Kikuchi, Y., Hida, W., Miki, H. & Shirato, K. 1995. Nitric oxide as a retrograde messenger in the nucleus tractus solitarii of rats during hypoxia. *J Physiol* 486, 495–504.

Ohta, A., Takagi, H., Matsui, T., Hamai, Y., Iida, S. & Esumi, H. 1993. Localization of nitric oxide synthase-immunoreactive neurons in the solitary nucleus and ventrolateral medulla oblongata of the rat: their relation to catecholaminergic neurons. *Neurosci Lett* 158, 33–35.

Ohtake, P.J., Torres, J.E., Gozal, Y.M., Graff, G.R. & Gozal, D. 1998. NMDA receptors mediate peripheral chemoreceptor afferent in put in the conscious rat. *J Appl Physiol* 84, 853–861.

Palmer, R.M., Rees, D.D., Ashton, D.S. & Moncada, S. 1988. L-arginine is the physiological precursor for the formation of nitric oxide in endothelium-dependent relaxation. *Biochem Biophys Res Commun* 153, 1251–1256.

de Paula, P.M. & Branco, L.G. 2003. Nitric oxide in the rostral ventrolateral medulla modulates hyperpnea but not anapyrexia induced by hypoxia. *Brain Res* 977, 231–238.

 doi: 10.1111/j.1748-1716.2006.01570.x

Powell, F.L., Huey, K.A. & Dwinell, M.R. 2000. Central nervous system mechanisms of ventilatory acclimatization to hypoxia. *Resp Physiol* **121**, 223–236.

Prabhakar, N.R., Kumar, G.K., Chang, C.H., Agani, F.H. & Haxhiu, M.A. 1993. Nitric oxide in the sensory function of the carotid body. *Brain Res* **625**, 16–22.

Qadri, F., Carretero, O.A. & Scicli, A.G. 1999. Centrally produced neuronal nitric oxide in the control of baroreceptor reflex sensitivity and blood pressure in normotensive and spontaneously hypertensive rats. *Jpn J Physiol* **81**, 279–285.

Reeves, S.R., Gozal, E., Guo, S.Z., Sachleben, L.R. Jr., Brittian, K.R., Lipton, A.J. & Gozal, D. 2003. Effect of long-term intermittent and sustained hypoxia on hypoxic ventilatory and metabolic responses in the adult rat. *J Appl Physiol* **95**, 1767–1774.

Reid, S.G. & Powell, F.L. 2005. The effects of chronic hypoxia on MK801-induced changes in the acute hypoxic ventilatory response. *J Appl Physiol* **99**, 2108–2114.

Reinhart, G.A., Lohmeier, T.E. & Mizelle, H.L. 1997. Temporal influence of the renal nerves on renal excretory function during chronic inhibition of nitric oxide synthesis. *Hypertension* **29**, 199–204.

Sato, K., Rodman, D.M. & McMurtry, I.F. 1999. Hypoxia inhibits increased ET_B receptor-mediated NO synthesis in hypertensive rat lungs. *Am J Physiol (Lung Cell Mol Physiol)* **276**, L571–L581.

Schmitt, P., Soulier, V., Pequignot, J.M., Pujol, J.F. & Denavit-Saubie, M. 1994. Ventilatory acclimatization to chronic hypoxia: relationship to noradrenaline metabolism in the rat solitary complex. *J Physiol* **477**, 331–337.

Schwenke, D.O., Pearson, J.T., Tsuchimochi, H., Mori, H. & Shirai, M. 2005. Exogenous nitric oxide centrally enhances pulmonary reactivity in the normal and hypertensive rat. *Clin Exp Pharmacol Physiol* **32**, 952–959.

Shapoval, L.N., Sagach, V.F. & Pobegailo, L.S. 1991. Nitric oxide influences ventrolateral medullary mechanisms of vasomotor control in the cat. *Neurosci Lett* **132**, 47–50.

Shirai, M., Pearson, J.T., Shimouchi, A., Nagaya, N., Tsuchimochi, H., Ninomiya, I. & Mori, H. 2003. Changes in functional and histological distributions of nitric oxide synthase caused by chronic hypoxia in rat small pulmonary arteries. *Br J Pharmacol* **139**, 899–910.

Spyer, K.M. 1994. Central nervous mechanisms contributing to cardiovascular control. *J Physiol* **474**, 1–19.

Subramanian, S., Erokwu, B., Han, F., Dick, T.E. & Strohl, K.P. 2002. L-NAME differentially alters ventilatory behavior in Sprague-Dawley and Brown Norway rats. *J Appl Physiol* **93**, 984–989.

Tagawa, T., Imaizumi, T., Harada, S., Endo, T., Shiramoto, M., Hirooka, Y. & Takeshita, A. 1994. Nitric oxide influences neuronal activity in the nucleus tractus solitarius of rat brainstem slices. *Circ Res* **75**, 70–76.

Vitagliano, S., Berrino, L., D'Amico, M., Maione, S., DeNovellis, V. & Rossi, F. 1996. Involvement of nitric oxide in cardiorespiratory regulation in the nucleus tractus solitarii. *Neuropharm* **35**, 625–631.

Wach, R.A., Bee, D. & Barer, G.R. 1989. Dopamine and ventilatory effects of hypoxia and almitrine in chronically hypoxic rats. *J Appl Physiol* **67**, 186–192.

Wada, Y., Matsuoka, H., Okuda, S. & Imaizumi, T. 1998. Chronic inhibition of nitric oxide in central nervous system does not cause hypertension. *Hypertens Res* **21**, 97–101.

Wang, Z.Z., Bredt, D.S., Fidone, S.J. & Stensaas, L.J. 1993. Neurons synthesizing nitric oxide innervate the mammalian carotid body. *J Comp Neurol* **336**, 419–432.

Wang, Z.Z., Stensaas, L.J., Bredt, D.S., Dinger, B. & Fidone, S.J. 1994. Localization and actions of nitric oxide in the cat carotid body. *Neuroscience* **60**, 275–286.

Weil, J.V. 1986. Ventilatory control at high altitude. In: M. Bethesda (ed.) *Handbook of Physiology. The Respiratory System. Control of Breathing*, pp. 703–728, American Physiological Society.

 doi: 10.1111/j.1748-1716.2006.01570.x